Stability Analysis of DC Microgrids With Switched Events

Vladimir Toro, Eduardo Mojica-Nava, Naly Rakoto-Ravalontsalama

Available online at www.sciencedirect.com

ScienceDirect

IFAC Papers Online CONFERENCE PAPER ARCHIVE

IFAC PapersOnLine 54-14 (2021) 221–226

Stability Analysis of DC Microgrids With Switched Events

Vladimir Toro * **Eduardo Mojica-Nava** **
Naly Rakoto-Ravalontsalama ***

* *Universidad Nacional de Colombia, Bogota, 111321, (e-mail: bwtorot@unal.edu.co).*
** *Universidad Nacional de Colombia, Bogota, 111321, (e-mail: eamojican@unal.edu.co)*
*** *IMT Atlantique, Nantes, France, 44307, (e-mail: naly.rakoto@imt-atlantique.fr)*

AbstractThis paper analyzes the stability of a direct current microgrid with a decentralized switched control using differential-algebraic equations and Lyapunov functions. The decentralized controllers regulate the voltage, achieve the power-sharing condition, and guaranty the non-Zeno condition. They also fulfill the droop-control condition for optimal power dispatch. The event of either connecting or disconnecting a converter is analyzed as a switched event. It is shown that the system is asymptotically stable under this class of switching events after either connecting or disconnecting a distributed generator.

Keywords: Microgrid, differential-algebraic equation, decentralized control, switched system.

1. INTRODUCTION

Distributed energy resources (DERs) have increasingly become attractive alternatives for energy generation, especially renewable sources. A direct current (DC) microgrid (MG) interconnects DERs that operate in DC through a common bus, each of them might have different power capacity and dynamical response Justo et al. (2013). Some of the main objectives of an isolated MG are voltage regulation, power-sharing or the condition that each converter shares power according to its maximum capacity, and the plug-and-play capacity which is the capacity of connecting or disconnecting a converter at an arbitrary time. Approaches for MG control can be classified as centralized, decentralized, and distributed Guerrero et al. (2011). Centralized controllers need a robust communication system and the changes in their structure require recalculate control parameters such as gains. A distributed controller allows flexibility; however, an appropriate communication network is also necessary. In a decentralized approach, several changes can be performed over the system parameters and the plug-and-play capacity is better compared with the other approaches because a complete communication system is not essential Meng et al. (2017).

The connection or disconnection of a DER implies abrupt changes in the MG's power, and voltages can generate jumps and impulse variations, endangering the components and loads and degrading the power quality Kumar et al. (2017). Switched events can be represented as a set of differential-algebraic equations (DAEs) to determine if there are impulses and jumps in the states. Examples for power systems are presented in Trenn (2009), Ñañez et al. (2017), Domínguez-García and Trenn (2010). In Trenn (2012), conditions for stability and solvability under switching are shown. In Domínguez-García and Trenn (2010), an analytical framework for jumps and impulse detection in switched systems with applications to power systems is presented. Passivity conditions to analyze switched systems are presented by Ñañez et al. (2017) including an example of an electrical system. A DAE model with the Lyapunov approach to control alternate current MGs is presented by De Persis et al. (2016), where algebraic conditions correspond to an equilibrium between demanded power and power set point. This approach does not consider switched events. Gross et al. (2018) consider failures or variations in the network's topology as switched events applied to electrical systems made of rotatory machines. Mojica-Nava et al. (2019) present a complete decentralized switched controller for a DC MG whose stability is proved using a passivity approach, the switched control commutes between two subsystems depending on the error of the generated voltage compared to a reference. At this article we extend the last approach to a switched event created when a converter is connected or disconnected to the MG. Also, an analysis of the Zeno behavior is performed because this fast transitions between subsystems endanger the components of the converter and degrade the power quality. Conditions for the existence of Zeno behavior are presented in Ames et al. (2005) for a class of system known as diagonal first quadrant (DFQ) hybrid systems. In Heymann et al. (2002) are presented the conditions for the existence of the Zeno set and Zeno executions.

The principal contribution of this paper is the analysis of a DC MG when DERs are connected or disconnected from a DAE's perspective, considering the space constraint, jump-free, and impulse-free conditions. Also, the stability of the controller is shown using Lyapunov functions. Jumps, impulses, and Zeno behavior are studied using

10.1016/j.ifacol.2021.10.356

the proposed switched control. Finally, the conditions for power-sharing and optimal power dispatch are presented.

The rest of this paper is organized as follows. Section 2 presents the electrical model for the microgrid with decentralized control and related Lyapunov functions. In Section 3, the connection of a converter to the MG is studied using tools for DAEs, stability is analyzed based on consistency space and projectors, and conditions for optimal dispatch are considered too. Simulation results are presented in Section 4. Finally, conclusions are presented in Section 5.

2. DC MICROGRID MODEL AND SWITCH CONTROL

For modeling the microgrid the next DC converter model based on current is presented

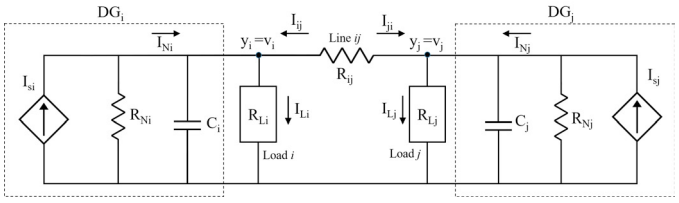

Figure 1. Two DC sources connected through a transmission line

Two converters are connected in parallel through a transmission line R_{ij} as shown in Figure 1. I_{si} is the current source, usually controlled by PWM (Pulse Width Modulation), R_{Ni} is the internal resistance of the source (which will be omitted assuming a very high value), and R_{Li} is the load for converter i. This model is extended to n parallel converters as follows

$$C_i\frac{dV_i}{dt} = I_{si} - \frac{V_i}{R_{Li}} + \sum_{j\in\mathcal{N}_i}^{n}\frac{1}{R_{ij}}(V_j - V_i) + u_i \qquad (1)$$

$$I_{ij} = \sum_{j\in\mathcal{N}_i}^{n}\frac{1}{R_{ij}}(V_j - V_i)$$

where C_i is the parallel capacitance for filtering, V_i is the voltage for DG$_i$, $\mathcal{N}_i$ represents the set of neighbors of node i, I_{ij} is the current between converter i and j, and u_i is the control term.

The next state-depending switching law is proposed by Mojica-Nava et al. (2019)

$$u_i = \begin{cases} \dfrac{P_{DGi}}{V_i} & \Delta V_i \geq 0 \\ \dfrac{P_{DGi} - k\Delta V_i^2}{V_i} & \Delta V_i < 0 \end{cases} \qquad (2)$$

where $\Delta V_i = V_{ref} - V_i$ is the difference between the voltage reference V_{ref} and the voltage at the i-th converter. $P_{DG_i} = V_i I_{si}$ is the power at the i^{th} converter, and k is a constant value for setting the effect of voltage variation, usually $0 < k \leq 1$.

Microgrid model assumptions: The voltage in the capacitors is strictly positive $V_i > 0$, and current sources are assumed to be stable and with a large enough internal resistance capable of supplying any load $R_{Ni} \longrightarrow \infty$.

The output of the system y_i is the voltage at each converter V_i, so expression (2) is a state-dependent switching control law with $y_i = V_i$. The feedback control law determines the current supplied by each source (Mojica-Nava et al. (2019))

$$u_i = -y_i \qquad (3)$$

To simplify (1) , we work with the admittance values given by $Y_{ij} = \frac{1}{R_{ij}}$. Connections are represented by a weighted Laplacian matrix L_w whose elements are defined by

$$L_{ij} = \sum_{j\in\mathcal{N}_{ij}}^{n} Y_{ij} \quad \text{if} \quad i = j \qquad L_{ij} = -Y_{ij} \quad if \quad i \neq j$$

with $Y_{ij} \neq 0$ and $Y_{Ni} = \frac{1}{R_{Ni}} \neq 0$. The load terms $Y_{Li} = \frac{1}{R_{Li}} =$ are included in the L_w matrix.

$$L_w = \begin{bmatrix} \sum_{j\in\mathcal{N}_{ij}}^{n} Y_{ij} & -Y_{12} & \cdots & -Y_{1n} \\ -Y_{21} & \sum_{j\in\mathcal{N}_{ij}}^{n} Y_{ij} & \cdots & -Y_{2n} \\ \vdots & \vdots & \ddots & \vdots \\ -Y_{n1} & -Y_{n2} & \cdots & \sum_{j\in\mathcal{N}_{ij}}^{n} Y_{ij} \end{bmatrix}$$

Defining the set of inputs I_{si} as the column vector given by $I_s = [I_{s1} \quad I_{s2} \quad \cdots \quad I_{sn}]^\top$. The system (1) without control input can be written in a matrix form as

$$\begin{aligned} C\dot{V} &= I_s - L_w V \\ I_{Ln} &= -L_w V \end{aligned} \qquad (4)$$

where $C \in R^{n\times n}$ is a diagonal matrix whose elements are the capacitance values C_i, and I_{Ln} is the line current I_{ij}.

Mojica-Nava et al. (2019) demonstrated the stability for system (4) based on a passivity approach. System (4) is asymptotically stable for closed-loop under switched control law (2) with Lyapunov function $H_p(v) = H_q(v)$ where v denotes the vector of voltages V, p and q denote the function before and after the switching event, respectively. Defining the Lyapunov function $H_p(v) = H_q(v) = \frac{1}{2}v^2$ for the close-loop system in both cases:

$\Delta V \geq 0$, replacing the value of $\dot{H}(v) = v\frac{dv}{dt}$

$$\dot{H} = V\left(\frac{I_s}{C} - \frac{L_w V}{C}\right) \leq 0$$

$$\dot{H} = V\left(\frac{-P_{DG}}{VC} - \frac{L_w V}{C}\right) \leq 0$$

$$\dot{H} = \frac{-P_{DG}}{C} - \frac{L_w V^2}{C} \leq 0$$

$$-P_{DG} - L_w V^2 \leq 0$$

$\Delta V < 0$

$$\dot{H} = V\left(\frac{-P_{DG} - k\Delta V^2}{VC} - \frac{L_w V}{C}\right) \leq 0$$

$$\dot{H} = -\frac{P_{DG}}{C} - \frac{\Delta V^2}{C} - \frac{L_w V^2}{C} \leq 0$$

$$-P_{DG} - \Delta V^2 - L_w V^2 \leq 0$$

In both cases, L_w represents the values of the positive-definite Laplacian matrix L_w, P_{DGi} are the positive power values of a diagonal matrix P_{DG} which is positive definite,

and k_i is a positive value. Then, $\dot{H}$ remains negative along the trajectories, $H_p(x) = H_q(x)$ are Lyapunov functions for the system, and the system is asymptotically stable.

Switched systems might present some behaviors exclusive for these systems. Transitions among subsystems depend on the states' conditions,the number of transitions is limited in a real model. However, when modeling it might occur an infinite number of transitions in a finite time, this is known as Zeno behavior or Zenoness (Heymann et al. (2005)).

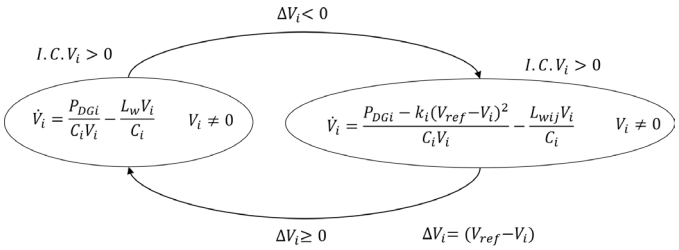

Figure 2. Converter switched control diagram

Definition 1. The existence of a nonempty Zeno set indicates the existence of a possible Zeno equilibrium (Zheng (2006)).

The Zeno set corresponds to the intersection of the domains of each subsystem. The sets are given by

$$S_1 : V_i \geq V_{ref} \quad S_2 : V_i < V_{ref}$$

The Zeno set is given by

$$Z_c = S_1 \cap S_2 = \{\emptyset\}$$

Then, the set Z_c is empty so there are not Zeno points in system (1) under switched control law (2).

3. DC MICROGRID UNDER SWITCH EVENT

Suppose a microgrid with n converters, then the switch S_i with $i = \{1, 2, \cdots, n\}$ is closed at $t = 0$s connecting the n^{th} converter to the MG through a transmission line Y_{ij} as shown in Figure 3. The weight values for converter n change depending on if it is connected or not. At $t < 0$s values $Y_{n,n}$ are set as zero, so all values for column n and row n are zero.

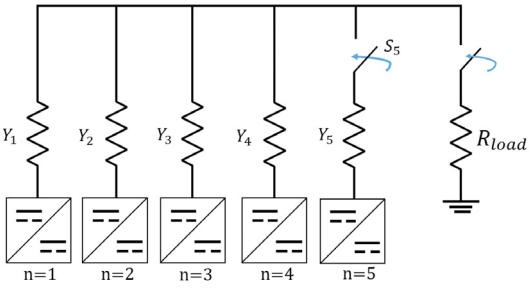

Figure 3. General diagram of a DC MG. The fifth converter is connected when the switch s_5 is closed

After the switch event, each converter updates its state variables according to Kirchhoff laws. The system is represented as a differential-algebraic system in the canonical form

$$E_{\sigma(t)}\dot{x}(t) = A_{\sigma(t)}x(t) + B_{\sigma(t)}u(t),$$

where $\sigma = \{1, 2, \cdots, p\}$ is the variable that represents the switch state, E_p, and $A_p \in \mathbb{R}^{n\times n}$, $B_p \in \mathbb{R}^{n\times m}$, $x \in \mathbb{R}^n$ is the state vector, and $u \in \mathbb{R}^m$ is the input vector (Trenn (2012)).

Definition 2. Admittance matrix The connection among converters at $t < 0$s is defined by the admittance matrix L_{w1}, at $t = 0$s an additional converter is (dis)connected with admittance matrix defined by L_{w2}.

Assumption 1: We assume the total number of converters is previously known, so $n-1$ converters are interconnected at $t < 0$s with $I_{Ln} = 0$, then at $t = 0$s converter n is connected.

The initial associated weight value changes from zero to a new value for that converter. System equations are presented before and after the switching event in a matrix form. The DAEs equations with pairs (E_1, A_1) and (E_2, A_2) are written in matrix form.

$t < 0$

$$\begin{bmatrix} C & 0 \\ 0 & 0 \end{bmatrix} \begin{bmatrix} \dot{V} \\ \dot{I}_{Ls} \end{bmatrix} = \begin{bmatrix} -L_{w1} & 0 \\ L_{w1} & I_s \end{bmatrix} \begin{bmatrix} V \\ I_{Ls} \end{bmatrix} + \begin{bmatrix} 1 \\ 0 \end{bmatrix} U_1 \qquad (5)$$

$t \geq 0$

$$\begin{bmatrix} C & 0 \\ 0 & 0 \end{bmatrix} \begin{bmatrix} \dot{V} \\ \dot{I}_{Ls} \end{bmatrix} = \begin{bmatrix} -L_{w2} & 0 \\ L_{w2} & I_s \end{bmatrix} \begin{bmatrix} V \\ I_{Ls} \end{bmatrix} + \begin{bmatrix} 1 \\ 0 \end{bmatrix} U_2 \qquad (6)$$

where U_1 is the vector of inputs $U_1 = [u_1 \quad u_2 \quad \cdots \quad u_{n-1}]$, and $U_2 = [u_1 \quad u_2 \quad \cdots \quad u_n]$.

The DAEs description already represents jumps and impulses. These are allowed in the system's solution by selecting an appropriate distributional framework Trenn (2012). Next, some important definitions for the switched system are given.

Definition 3. Regularity (Trenn (2012)). Matrix pairs (E_1, A_1), (E_2, A_2), $\cdots, (E_n, A_n)$ are regular if the pencil $(sE_\sigma - A)$ is regular, it means if $\det(sE - A)$ is a polynomial different from zero. This condition guarantees that the switched system always has a solution, no matter the initial value.

This condition is fulfilled by systems (5) and (6) whose determinants are given by $\Delta_1 = -sC - L_{w1}$ and $\Delta_2 = -sC - L_{w2}$.

Definition 4. Consistency space and projectors (Liberzon and Trenn (2012)). Solutions for the switched system are given inside a space known as the consistency space. Matrices pairs (E_i, A_i) are regular if they can be represented in the quasi-Weierstrass form.

The Wong sequences give an algorithmic way to determine the quasi-Weierstrass form. The consistency projectors $\Pi_{(E,A)}$, the differential projectors $\Pi^{\text{diff}}_{(E,A)}$, and the impulse projectors $\Pi^{\text{imp}}_{(E,A)}$ are defined by Trenn (2012). Those are calculated for systems (5) and (6) as follows

$$\Pi_{(E_1,A_1)} = I_{2n\times 2n} \qquad \Pi_{(E_2,A_2)} = I_{2n\times 2n}$$

Then, the space is consistent.

Definition 5. Impulse-free (Trenn (2012)). A switched system defined by a set of DAEs, with regular matrix pairs (E_p, A_p) cannot produce an impulse for all solutions if the following impulse-free condition holds:

$$E_q(I-\Pi_q)\Pi_p = 0$$

Definition 6. Sufficient condition for jump free (Trenn (2009)):

$$(I-\Pi_q)\Pi_p = 0.$$

Definition 7. Condition for inputs Ñañez et al. (2017). For each $\sigma \in \Sigma$,

$$\Pi_\sigma^{imp} B_\sigma = 0$$

Definition 8. Stability condition for switched systems Trenn (2012). For a switched DAE with regular pairs $(E_p, A_p) \in \{1, \cdots, \bar{p}\}$, and consistency projectors Π_{E_p,A_P}, the system is asymptotically stable for all switching signals if

1) $E_p\dot{x} = A_p x$ is asymptotically stable with Lyapunov function H_p,

2) Fulfills the impulse-free condition $E_q(I-\Pi_q)\Pi_p = 0$ for all $q \in (1, ..., p)$, and

3) $H_q(\Pi_q x) \leq H_p(x)$ for all $x \in \mathcal{H}_p^*$=imΠ_p.

Theorem 9. Consider the switched system represented by DAEs (5) and (6) with decentralized control (2) with regular matrix pairs (E_1, A_1), (E_2, A_2), and Lyapunov functions H_p and H_q. If the system satisfies the conditions of definition (8), then the system is asymptotically stable.

Proof. The impulse-free condition is satisfied for both subsystems

	$q=1$	$q=2$
$p=1$	$E_q(I-\Pi_p)\Pi_p = 0$	$E_q(I-\Pi_p)\Pi_p = 0$
$p=2$	$E_q(I-\Pi_p)\Pi_p = 0$	$E_q(I-\Pi_p)\Pi_p = 0$

And the jump condition (8) $H_q(\Pi_q x) \leq H_p(x)$ is fulfilled for the Lyapunov function, with $1/2(\Pi_q x)^2 < H_p(x)$. Then the system is asymptotically stable.

3.1 Optimal Control Criteria and Power Sharing

Different resistance values at each transmission line cause that voltages differ from the load side compared with the output side at each converter. That results in poor voltage regulation and insufficient power-sharing which is fulfilled achieving the next condition

$$\frac{P_i}{P_{max,i}} = \cdots = \frac{P_j}{P_{max,j}}. \tag{7}$$

If the reference voltage is achieved as $t \to \infty$, the last expression can be rewritten as $\frac{I_i}{I_{max,i}} = \cdots = \frac{I_j}{I_{max,j}}$, which is an equilibrium among each source. Defining value $r_i = \frac{1}{I_{max,i}}$, power sharing condition is equal to $r_i I_i = \cdots = r_j I_j$ or $r_i P_i = \cdots = r_j P_j$.

Optimal control for MGs solves the problem of dispatching DERs based on its marginal cost and availability. It is not always desirable that a source supplies power according to its maximum capacity. Sometimes a converter can have major priority over others to reduce the cost of power generation. This requirement corresponds to a cost minimization problem with restrictions.

Theorem 10. Assume that system defined by (1) is asymptotically stable with control law (2), where each source has a dispatch factor r_i. Then, the power-sharing condition is also the optimal power dispatch condition for the system, this means the optimal power to be delivered for each converter to supply the demand according the maximum power capacity at each converter.

Proof. In steady-state, the equilibrium equation is given by

$$U - L_w V = 0, \tag{8}$$

Assuming a quadratic cost function given by $u_c = \sum_{i\in N} \frac{1}{2} r_i u_i^2$, subject to (8). Applying the Lagrange multipliers method, we have the next equation

$$L(u, v, \lambda) = \sum_{i\in N} r_i u_i^2 + \lambda(u - L_w V), \tag{9}$$

with $\nabla L_u = \sum_{i\in N} r_i u_i + \lambda = 0$, $\nabla L_v = -\lambda(-L_w) = 0$, and $\nabla L_\lambda = u - V(-L_w) = 0$. Matrix $-L_w$ can be written as an admittance matrix that includes the values of the local loads. Then, the solution of $\nabla L_\lambda = u - V(-L_w) = 0$ are the set of values $\lambda = c\mathbf{1}_n$, with $c \in \mathbb{R}$. Then, the condition for the optimal control input is given by

$$u_i = -\frac{c}{r_i}, \tag{10}$$

Then, the optimal input value for the i^{th} converter is given as a function of constant c over the cost value r_i. Where $c\sum_{i\in N} \frac{1}{r_i} = \sum_{i\in N} I_{si} + \sum_{i\in N} I_L$ (Zhao and Dörfler (2015)). As control (2) acts as a droop control in two states, being the same as $\Delta V = 0$, optimal condition (10) is fulfilled, and the theorem is demonstrated.

4. SIMULATION RESULTS

A five converter DC microgrid is simulated in Simulink considering two cases as follows

4.1 Case 1

The DC MG is simulated using the model of Figure 3, four interconnected converters share power, a linear load is connected at $t = 0.2$s, then a fifth converter ($n = 5$) is connected at $t = 0.4$s. The MG parameters are shown in Table 1.

Table 1. MG parameters

Converter	1	2	3	4	5
Maximum Active Power (W)	360	330	300	270	240
Line Resistor R_i (Ω)	0.64	0.50	0.90	0.70	0.82
Output Capacitor			2.2mF		
V_{ref}			80V		
k			$10\Omega^{-1}$		
Local load			5.0 Ω		

The Weighted Laplacian matrix is given by L_w

$$L_w = \begin{bmatrix} -13.77 & 3.56 & 2.67 & 2.99 & 2.78 & 1.76 \\ 3.56 & -15.52 & 3.11 & 3.42 & 3.21 & 2.20 \\ 2.67 & 3.11 & -11.96 & 2.53 & 2.33 & 1.31 \\ 2.99 & 3.42 & 2.53 & -13.23 & 2.64 & 1.62 \\ 2.78 & 3.21 & 2.33 & 2.64 & -12.39 & 1.41 \\ 1.76 & 2.20 & 1.31 & 1.62 & 1.41 & -8.32 \end{bmatrix}$$

Figure 4 shows the voltage at each converter. A load is connected at $t = 0.2$s, and converter five is connected at

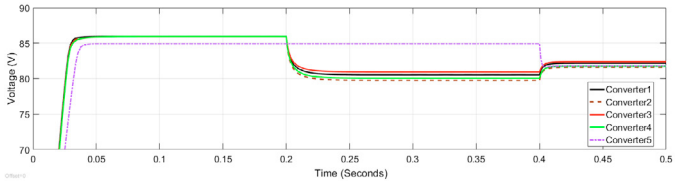

Figure 4. Voltage output at each converter for Case 1

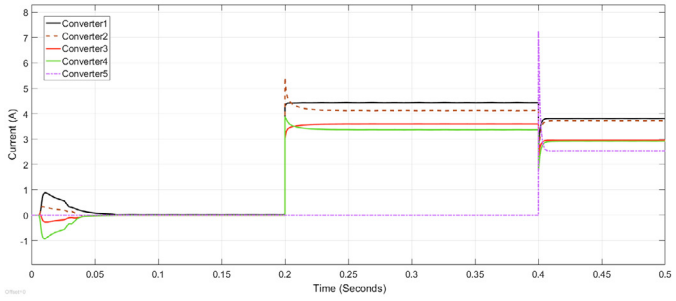

Figure 5. Current measured at each converter for Case 1

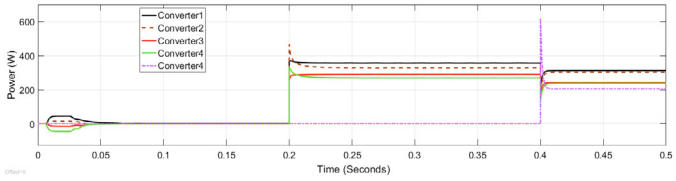

Figure 6. Power Sharing Among Converters for Case 1

$t = 0.4$s. Notice the difference in the voltage regulation before and after connecting the load. Also, voltage regulation improves when the fifth converter is connected. The generated voltage does not present peaks or jumps. Figure 5 and Figure 6 show the current and power at each converter, respectively. The current and power-sharing condition is achieved. There are current peaks because of the load connections, but mostly because of the fifth converter's connection.

4.2 Case 2

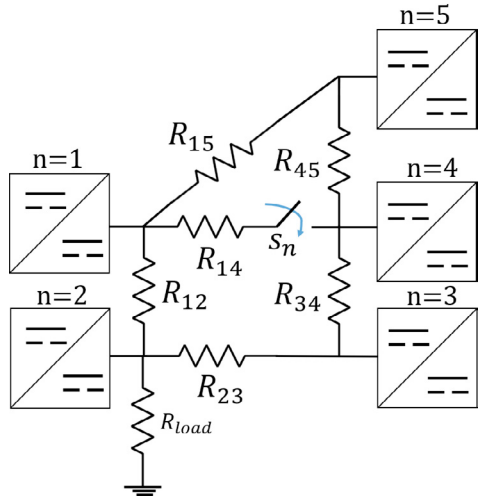

Figure 7. Second case MG model

Here, the MG has the configuration presented in Figure 7. A linear load is connected to the second converter at $t = 0$s. The interrupter is closed at $t = 0.3$s connecting the fourth and fifth converters. The parameters of the MG are shown in Table 2, and the physical connections are represented by matrices L_{w1} and L_{w2} for the instants before and after closing s_n, respectively.

Table 2. MG parameters

Converter	1	2	3	4	5
Maximum Active Power (W)	360	330	300	270	240
Line Resistor R_i (Ω)	0.64	0.50	0.90	0.70	0.82
Output Capacitor			2.2mF		
V_{ref}			80V		
k			$10\Omega^{-1}$		
Local load			5.0 Ω		
$R_{12} = R_{23} = R_{34} = R_{45} = R_{15}$			0.1 Ω		

$$L_{w1} = \begin{bmatrix} -1.8333 & 0.8333 & 0 & 0 & 1.0000 \\ 0.8333 & -1.2878 & 0.4545 & 0 & 0 \\ 0 & 0.4545 & -1.7045 & 1.2500 & 0 \\ 0 & 0 & 1.2500 & -2.5833 & 1.3333 \\ 1.0000 & 0 & 0 & 1.3333 & -2.3333 \end{bmatrix}$$

$$L_{w2} = \begin{bmatrix} -3.8333 & 0.8333 & 0 & 2.0000 & 1.0000 \\ 0.8333 & -1.2878 & 0.4545 & 0 & 0 \\ 0 & 0.4545 & -1.7045 & 1.2500 & 0 \\ 2.0000 & 0 & 1.2500 & -.5833 & 1.3333 \\ 1.0000 & 0 & 0 & 1.3333 & -2.3333 \end{bmatrix}$$

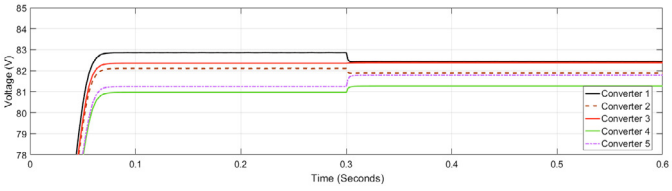

Figure 8. Voltage output at each converter for Case 2

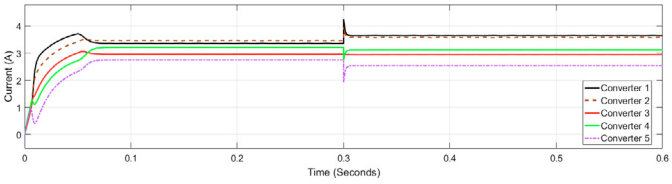

Figure 9. Current output at each converter for Case 2

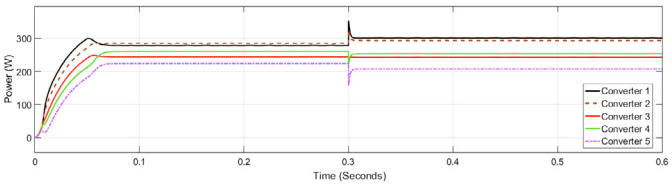

Figure 10. Power measured at each converter for Case 2

The voltage at each converter is shown in Figure 8. The load is connected at $t = 0$s, and the fifth converter is connected at $t = 0.3$s. After the system starts, voltage outputs stabilize in $t < 0.1$s, as expected voltage regulation improves when the fifth converter is connected. Voltage output presents neither peaks nor oscillations. The power-sharing condition is kept, as shown in Figure 9 and

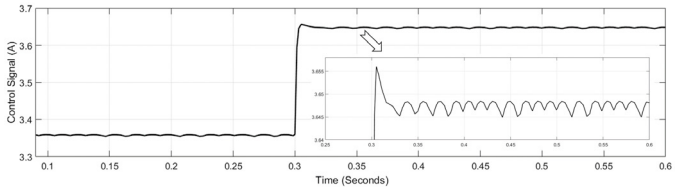

Figure 11. Control signal applied at the first converter for Case 2

Figure 10. However, as in the first case, voltage regulation is not as good as expected. There is a trade between power sharing and voltage regulation as shown in Mojica-Nava et al. (2019), and depends directly on selecting the factor k. Figure 11 shows the control signal at the first converter it changes at $t = 0.3$s when the additional converter is connected and presents a small ripple because of the switching.

5. CONCLUSION

A DC MG with a decentralized controller was modeled as a DAEs problem when an additional converter was connected or disconnected. Stability, impulse-free, and jump-free conditions were demonstrated. Stability for the controller was proved using a Lyapunov functions approach, and also non-Zeno behavior was verified. It was checked that variations over the network's topology when converters are connected could also be analyzed using the DAEs approach. It was demonstrated that the decentralized control fulfills the power-sharing condition. Also, the conditions for optimal power dispatch were presented.

REFERENCES

Ñañez, P., Sanfelice, R.G., and Quijano, N. (2017). Notions and a passivity tool for switched dae systems. In *2017 IEEE 56th Annual Conference on Decision and Control (CDC)*, 3612–3617.

Ames, A.D., Abate, A., and Sastry, S. (2005). Sufficient conditions for the existence of zeno behavior. In *Proceedings of the 44th IEEE Conference on Decision and Control*, 696–701.

De Persis, C., Monshizadeh, N., Schiffer, J., and Dörfler, F. (2016). A lyapunov approach to control of microgrids with a network-preserved differential-algebraic model. In *2016 IEEE 55th Conference on Decision and Control (CDC)*, 2595–2600.

Domínguez-García, A.D. and Trenn, S. (2010). Detection of impulsive effects in switched daes with applications to power electronics reliability analysis. In *49th IEEE Conference on Decision and Control (CDC)*, 5662–5667.

Gross, T., Trenn, S., and Wirsen, A. (2018). Switch induced instabilities for stable power system DAE models. *IFAC-PapersOnLine*, 51(16), 127–132.

Guerrero, J.M., Vasquez, J.C., Matas, J., De Vicuña, L.G., and Castilla, M. (2011). Hierarchical control of droop-controlled AC and DC microgrids - A general approach toward standardization. *IEEE Transactions on Industrial Electronics*, 58(1), 158–172.

Heymann, M., Lin, F., Meyer, G., and Resmerita, S. (2002). Analysis of zeno behaviors in hybrid systems. *Proceedings of the IEEE Conference on Decision and Control*, 3(December), 2379–2384. doi: 10.1109/cdc.2002.1184191.

Heymann, M., Lin, F., Meyer, G., and Resmerita, S. (2005). Analysis of Zeno behaviors in a class of hybrid systems. *IEEE Transactions on Automatic Control*, 50(3), 376–383. doi:10.1109/TAC.2005.843874.

Johansson, K.H., Egerstedt, M., Lygeros, J., and Sastry, S. (1999). On the regularization of Zeno hybrid automata. *Systems and Control Letters*, 38(3), 141–150. doi: 10.1016/S0167-6911(99)00059-6.

Justo, J.J., Mwasilu, F., Lee, J., and Jung, J.W. (2013). AC-microgrids versus DC-microgrids with distributed energy resources: A review. *Renewable and Sustainable Energy Reviews*, 24, 387–405.

Kumar, D., Zare, F., and Ghosh, A. (2017). DC Microgrid Technology: System Architectures, AC Grid Interfaces, Grounding Schemes, Power Quality, Communication Networks, Applications, and Standardizations Aspects. *IEEE Access*, 5, 12230–12256.

Liberzon, D. and Trenn, S. (2012). Switched nonlinear differential algebraic equations : Solution theory , Lyapunov functions , and stability. *Automatica*, 48(5), 954–963.

Meng, L., Shafiee, Q., Trecate, G.F., Karimi, H., Fulwani, D., Lu, X., and Guerrero, J.M. (2017). Review on Control of DC Microgrids and Multiple Microgrid Clusters. *IEEE Journal of Emerging and Selected Topics in Power Electronics*, 5(3), 928–948.

Mojica-Nava, E., Rey, J.M., Torres-Martinez, J., and Castilla, M. (2019). Decentralized Switched Current Control for DC Microgrids. *IEEE Transactions on Industrial Electronics*, 66(2), 1182–1191.

Trenn, S. (2009). Regularity of distributional differential algebraic equations. *Mathematics of control, signals, and systems*, 21(3), 229.

Trenn, S. (2012). *Switched Differential Algebraic Equations*, 189–216. Springer London, London.

Zhao, J. and Dörfler, F. (2015). Distributed control and optimization in DC microgrids. *Automatica*, 61, 18–26.

Zheng, H. (2006). Simulating zeno hybrid systems beyond their zeno points. Technical report, Technical Report No. UCB/EECS-2006-114.